# Nutrient Dynamics of the Upwelling Area in the Changjiang Estuary

**Shaofeng Pei, Zhiliang Shen and Edward A. Laws**

**Abstract** Nutrient dynamics and its influence on the distribution of chlorophyll-a in the upwelling area of the Changjiang (Yangtze) River estuary were investigated in the spring (May) and summer (August) of 2004. The spring upwelling was apparent in the region of 122°20′–123°00′ E, 31°00′–32°00′ N and was associated with low temperature (16–21 °C), high salinity (24–33), and low dissolved oxygen (2.5–6.0 mg $L^{-1}$) in the upper 10 m of the water column. The spring upwelling increased the mixed-layer phosphate, nitrate, and silicate concentrations to roughly 1, 15, and 15 μmol $L^{-1}$, respectively, and improved the light transparency in the euphotic zone. This improvement in phytoplankton-growing conditions was followed by an increase in chlorophyll-a concentrations. The summer upwelling was weaker and occurred over a smaller geographical area (122°20′–123°00′ E, 31°15′–31°50′ N). Strongly influenced by turbid Changjiang diluted water (CDW), it had little impact on the upper 10 m of the water column but instead increased nutrient concentrations at greater depths. The high concentration of particulates in the CDW reduced light transmission in the upper 10 m and, hence, limited phytoplankton growth throughout the water column. Chlorophyll-a concentrations in the summer upwelling area were roughly an order of magnitude lower than in the spring. Water clarity, as influenced by the CDW, appears to be the principal factor limiting the impact of upwelling on phytoplankton biomass in this area.

**Keywords** Upwelling · Dynamics · Nutrient · Chlorophyll-*a* · Transparency Phytoplankton · Changjiang estuary

Z. Shen (✉)
Key Laboratory of Marine Ecology and Environmental Sciences, Institute of Oceanology, Chinese Academy of Sciences, Qingdao 266071, China
e-mail: zhlshen@qdio.ac.cn

S. Pei
Key Laboratory of Coastal Wetlands, China Geological Survey, Qingdao Institute of Marine Geology, Ministry of Land & Resources, Qingdao 266071, China

E. A. Laws
Department of Oceanography and Coastal Sciences, School of the Coast and Environment, Louisiana State University, Baton Rouge 70803, USA

 
Z. Shen (ed.), *Studies of the Biogeochemistry of Typical Estuaries and Bays in China*, Springer Earth System Sciences, https://doi.org/10.1007/978-3-662-58169-8_6

Upwelling is important to the ecology of coastal marine ecosystems and ultimately to fish production (Cui and Street 2004; Oleg et al. 2003; Ryther 1969) because it can bring nutrients from intermediate depths into the euphotic zone and hence stimulate the phytoplankton community and primary production (Blasco et al. 1980, 1981; Margalef 1978a, b). Numerous previous studies have explored the dynamics and impacts of upwelling systems (e.g., Barber and Smith 1981; Smith et al. 1983). Most recently, Ramírez et al. (2005) reported an intense wind-driven spring upwelling event in the NW Alboran Sea, which temporally eased the nitrogen (N) limitation of the phytoplankton community, and Skliris and Djenidi (2006) pointed out that the upwelling of nitrate-rich deep water, both upstream and downstream of a submarine canyon off the NW Corsican coast, enhanced local primary production.

Coastal upwelling occurs along many parts of the Chinese coast and especially in the East China Sea. Hu (1994) anticipated the existence of summer upwelling there in an area between 27°30′ N and 30°30′ N and bordering 124°00′ E. Chen et al. (2004) surveyed the upwelling between 26°00′ N and 30°30′ N in the East China Sea during the summer of 1998 and evaluated the effects of the upwelling on primary production and nitrate-based new production. Wang and Wang (2007) studied the seasonal variations of coastal upwelling on the inner shelf of the East China Sea and estimated nutrient fluxes into the euphotic zone during the summer upwelling period.

In recent years, frequent outbreaks of red tides in the East China Sea have become a growing concern (Chen et al. 2003; Wang 2006). About 75% of those outbreaks have taken place in the Changjiang (Yangtze) River estuary (122°15′–123°10′ E, 30°30′–32°00′ N) (Chen et al. 2003). However, the upwelling in this area has received less attention than the well-known summer coastal upwelling in the East China Sea between 26°00′ N and 30°30′ N (Chen et al. 1999, 2004; Zhou et al. 2003). Upwelling in the estuary has been observed and documented since the early 1980s (Beardsley et al. 1983; Limeburner et al. 1983; Yu et al. 1983). Persistent upwelling in the region of 122°20′–123°10′ E, 31°00′–32°00′ N has been observed from May to August (Zhao 1993; Zhao et al. 1992, 2001). Zhao et al. (2001) concluded that summer upwelling in the estuary could transport high concentrations of nitrate, phosphate, and silicate into the upper 10 m of the water column, and the physical dynamics of this summer upwelling have been simulated mathematically (Pan and Sha 2004; Zhu 2003; Zhu et al. 2003b). There is little information, however, on the dynamics of nutrients or their influence on the distribution of chlorophyll-*a* (Chl-*a*) in the Changjiang River estuary during either the spring or summer upwelling periods.

In this section, we report data collected during two cruises to the Changjiang River estuary during May and August 2004 to quantify the impact of upwelling on the ecology of this ecosystem. The distributions of nutrients and nutrient structure, their effect on Chl-*a* concentrations, and the seasonal difference in Chl-*a* distributions were investigated. In addition, we estimated nutrient fluxes into the euphotic zone during the spring upwelling period and summarized spatial variations of hydrological parameters in the upwelling area as a reference for future studies concerned with the increasingly serious eutrophication and occurrence of harmful algal blooms in the Changjiang River estuary.

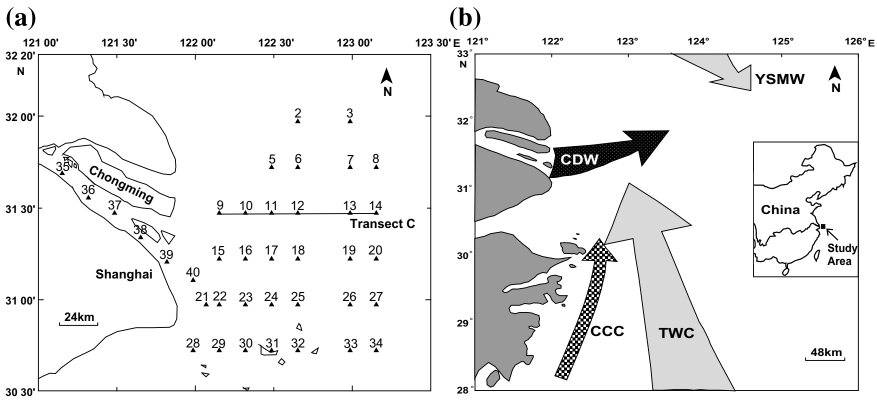


**Fig. 1** **a** Sampling stations in the Changjiang estuary; **b** Distribution of water masses in Changjiang coastal area: TWC, Taiwan warm current; CDW, Changjiang diluted water; YSMW, Yellow sea mixing water; CCC, China coastal current

## 1 Study Area and Methods

The study area and sampling stations are shown in Fig. 1a. The current system in the area is complex (Katoh et al. 2000; Naimie et al. 2001; Su 1998; Zhang and Wang 2004), with two major currents, the Changjiang diluted water (CDW) and Taiwan warm current (TWC) (Fig. 1b), interacting and causing nutrient freshening and redistribution (Guo et al. 2003). These current interactions are modified locally by several other minor water masses: the China coastal current (CCC), the Yellow Sea mixing water (YSMW), and the Yellow Sea cold water mass (Zhou et al. 2003).

The CDW, as the name indicates, is the result of mixture of Changjiang River water with seawater in the deltaic region, which is rich in nutrients derived from land runoff. The CDW flows generally toward the northeast from May to October as indicated in Fig. 1b (Zhu 2003). The nutrient loads from the river have increased dramatically in past two decades as a result of the overuse of fertilizer and ill-managed discharges of industrial and household sewage (Gao and Song 2005; Shen et al. 2001; Wang 2006).

The TWC is characterized by high salinities (>29), temperatures ranging from 16 to 29.5 °C (Chen et al. 2003), and low dissolved oxygen (DO) concentrations. In the summer, the TWC originates mainly in the Taiwan Strait, but in the winter, most of the TWC originates in the Kuroshio Current, which moves onto the East China Sea shelf northeast of Taiwan (Chen and Sheu 2006). The TWC is rich in nutrients and a major source of nutrients in the study area (Zhou et al. 2003).

In summer, the TWC flows directly northeastward, passes through the Changjiang coastal area, reaches near 32°N, and induces upwelling in the Changjiang estuary (Bai and Hu 2004; Zhao 1993; Zhao et al. 1992, 2001; Zhu 2003). The upwelling in the study area is driven by several factors, including winds, submarine topography, and currents. In general, the flow of the TWC as it moves northward along the slope of the submerged river valley off the mouth of the Changjiang River is primarily responsible for the upwelling, in combination with submarine topography and baroclinic effects resulting from the mixing of river water and seawater (Zhao 1993; Zhu 2003).

Cruises were carried out in May and August of 2004 to the Changjiang estuary and adjacent coastal waters. Water samples from 38 stations (Fig. 1a) were collected with Nansen samplers at depths of 0, 5, 10, 20, and 30 m and within the bottom layer of the water column and were then filtered through pre-combusted (450 °C for 6 h) Whatman GF/F filters (25 mm in diameter). Afterward, all samples were preserved with 0.3% chloroform in polyethylene bottles pretreated with 1:10 hydrochloric acid by volume for 24 h and then stored in an icebox at −25 °C before laboratory analysis.

Nutrients and Chl-*a* were measured using the methodologies of Shen et al. (2006), and DO using the Winkler method. Dissolved inorganic nitrogen (DIN) was calculated as the sum of $NO_3$–N, $NO_2$–N, and $NH_4$–N.

## 2 Nutrient Dynamics of the Upwelling Area in Spring

In the spring of 2004, river runoff increased sharply from an average of 18,000 $m^3$ $s^{-1}$ in April to 35,700 $m^3$ $s^{-1}$ in June as recorded at the Datong Hydrographic Station, which is located at the tidal limit of the Changjiang estuary, approximately 650 km upstream from the river mouth. This discharge was associated with a large influx of nutrients into the coastal zone. Profiles of temperature (T), salinity (S), and DO were used to determine the extent of coastal upwelling. The distribution of nutrients, nutrient ratios, and Chl-*a* in the upwelling area was examined as a function of depth (vertical profiles) and horizontally in typical water layers.

### *2.1 Vertical Distributions of Nutrient and Nutrient Ratio*

Transect C (31°30′ N, Fig. 1a) was found to be representative with respect to system characteristics. Upwelling is evidenced by concave isolines of T, S, and DO along 122°20′–123°00′ E (Fig. 2a, c). Isotherms, between 16.5 and 20 °C, rise from the bottom toward the surface (Fig. 2a); the 16.5 °C line extends from ~30 to ~10 m; and the 19.5 °C isotherm extends almost to the surface. Isohalines ranging from 30 to 33 also show notable concavity; the 33 isohaline rises from almost 30 to 10 m (Fig. 2b). Dissolved oxygen isolines between 2.5 and 4 mg $L^{-1}$ are notably concave (Fig. 2c), and the 4 mg $L^{-1}$ isoline rises from ~15 to < 5 m. The direction of gradients between the isolines indicates that upwelled water is characterized by low temperature, high salinity, and low DO along 122°20′–123°00′ E and that this water reaches the euphotic zone above 5 m in the spring. Zhao (1993) documented similar phenomena. Moreover, influenced by upwelling, the thermocline shoaled by 10 m and became thinner (Fig. 2a), and there was virtually no mixed layer in the region of most intense upwelling.

Upwelling clearly influenced the distribution of nutrients (Fig. 2d, i). The enrichment of near-surface waters with upwelled phosphate ($PO_4$–P) (Fig. 2d) resulted in closed elliptical phosphate isocontours between depths of ~25 and 8 m and longitudes of 122°25′ E to 122°38′ E. Peak $PO_4$–P concentrations were greater than 1.05 $\mu$mol $L^{-1}$, which is much higher than the concentration of ~0.5 $\mu$mol $L^{-1}$ in waters surrounding the region of upwelling.

The distributions of nitrate ($NO_3$–N) and silicate ($SiO_3$–Si) were similar to that of $PO_4$–P with one noteworthy exception: The concentrations of $NO_3$–N and $SiO_3$–Si in the upwelled water were lower than the corresponding concentrations in the CDW (Fig. 2e, f). As a result, surface water $NO_3$–N and $SiO_3$–Si concentrations declined more or less monotonically in an onshore–offshore direction along Transect C, whereas $PO_4$–P concentrations peaked over the center of upwelling. This pattern contrasts with the earlier work of Zhao et al. (2001), which characterized the upwelling core as a center of maximum inorganic nutrient concentrations. This appears to be true for $PO_4$–P but not for $NO_3$–N and $SiO_3$–Si. Upwelled waters contained 13–18 $\mu$mol $L^{-1}$ and 17–20 $\mu$mol $L^{-1}$ of $NO_3$–N and $SiO_3$–Si, respectively, much lower than the corresponding concentrations in the CDW. The offshore transport of upwelled water did, however, produce a clearly discernible maximum in $NO_3$–N and $SiO_3$–Si at longitude 122°40′ E at a depth of ~5 m (Fig. 2e, f).

Dissolved inorganic nitrogen (DIN): $PO_4$–P ratios were relatively high (>40) in the CDW compared with upwelled water (<20) and offshore water (~20). There was consequently a more or less monotonic onshore–offshore decline in surface water DIN: $PO_4$–P ratios and a local minimum between roughly 10 and 30 m in the upwelling core (Fig. 2g). $SiO_3$–Si: DIN ratios, on the other hand, were lowest in the CDW water (<0.8) and highest in offshore water (~2.8). There was, consequently, a monotonic onshore–offshore increase in $SiO_3$–Si: DIN ratios and a localized maximum at depths of 10–20 m in the core of the upwelled water (Fig. 2h). The $SiO_3$–Si: $PO_4$–P ratios were lowest in upwelled water (~16) and highest in offshore water (~50). There was, consequently, a local minimum of $SiO_3$–Si: $PO_4$–P ratios in the core of the upwelled water at a depth of 10–15 m and a more or less monotonic onshore–offshore increase in surface water $SiO_3$–Si: $PO_4$–P ratios, punctuated by a local minimum near the center of the upwelling region (Fig. 2i).

Inorganic nutrient concentrations are not conservative quantities, and in this system, phytoplankton uptake had a discernible effect on nutrient concentrations within the euphotic zone in the vicinity of upwelling. Maximum Chl-*a* concentrations were ~16 $\mu$g $L^{-1}$ (Fig. 2j). Assuming C:N and C:P ratios of 5.7 and 41 by weight, respectively (Redfield et al. 1963), and a C: Chl-*a* ratio of ~40 by weight (Riemann et al. 1989), a Chl-*a* concentration of 16 $\mu$g $L^{-1}$ would be associated with phytoplankton N and P concentrations of 8 and 0.5 $\mu$mol $L^{-1}$, respectively. Thus, phytoplankton uptake very likely accounts for much of the vertical gradient in $PO_4$–P between the subsurface maximum of ~1.05 $\mu$mol $L^{-1}$ and the surface concentration of ~0.6 $\mu$mol $L^{-1}$ directly over the center of upwelling (Fig. 2d). Along Transect C surface Chl-*a* concentrations increased from 10 $\mu$g $L^{-1}$ in the CDW to ~16 $\mu$g $L^{-1}$ over the center

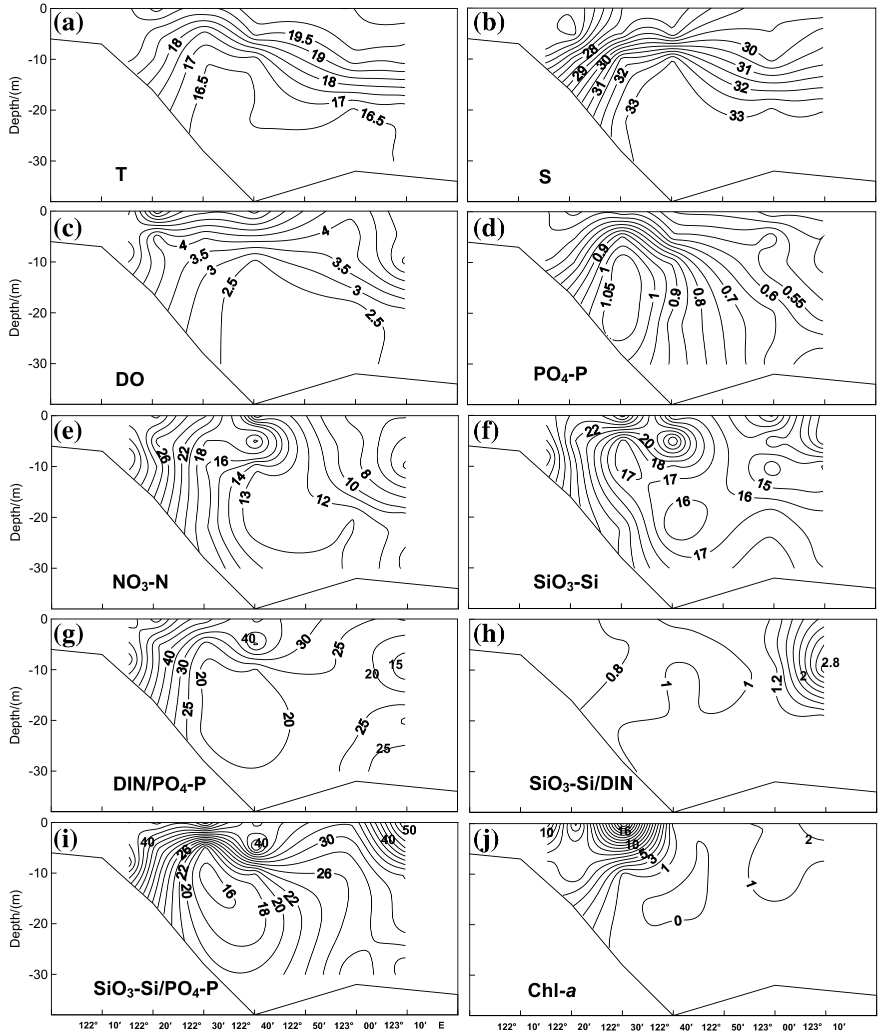


**Fig. 2** Vertical distributions of temperature (T), salinity (S), dissolved oxygen (DO), nutrients, nutrient ratios, and chlorophyll-*a* (Chl-*a*) in Transect C in spring: **a** T (°C); **b** S; **c** DO (mg $L^{-1}$); **d** $PO_4$–P (μmol $L^{-1}$); **e** $NO_3$–N (μmol $L^{-1}$); **f** $SiO_3$–Si (μmol $L^{-1}$); g DIN: $PO_4$–P; h $SiO_3$–Si: DIN; i $SiO_3$–Si: $PO_4$–P; j Chl-*a* (μg $L^{-1}$)

of upwelling. Nitrate concentrations along this same segment of the transect declined from ~26 to ~18 μmol $L^{-1}$. Roughly half of this decrease in $NO_3$–N was probably due to phytoplankton uptake.

## 2.2 Horizontal Distributions of Nutrient and Nutrient Ratio

The areal extent of the influence of upwelling is clearly shown in the horizontal pattern of water column properties at a depth of 10 m (Fig. 3). Upwelling of relatively cold and salty water with a low DO concentration is apparent in the area 122°20′–123°00′ E, 31°00′–32°00′ N, which includes Transect C (31°30′ N). A large, cooler area is evidenced by semienclosed isotherms of (<16.5–18 °C), whereas temperatures in the surrounding area were >18.5 °C (Fig. 3a). An onshore–offshore increase in salinity was punctuated by a local maximum of >32 at the center of upwelling (122°40′ E, 31°30′ N) and closed isohalines at 31 and 32 (Fig. 3b), consistent with an earlier report by Zhu et al. (2003a). Isocontours of DO between <2.5 mg $L^{-1}$ and 3.5 mg $L^{-1}$ formed ellipses around a minimum DO of ~2 mg $L^{-1}$, much lower than the DO of >4 mg $L^{-1}$ in the surrounding area (Fig. 3c). The pattern of DO isolines is very similar to the pattern of isotherms in Fig. 3a. Moreover, horizontal extensions of isotherms, isohalines, and DO isolines indicate that the upwelling water extended into the area north of 32°00′ N.

Within the upper 10 m of the water column, both physical and biological processes influenced inorganic nutrient concentrations, but at depths ≤10 m, phytoplankton concentrations were too low to have a significant impact on the distribution of nutrients (Fig. 2j). At the surface, a large area with $PO_4$–P concentrations as high as 0.7–1.0 μmol $L^{-1}$ appeared near the river mouth, whereas in the upwelling area, surface $PO_4$–P concentration was lower (0.4–0.6 μmol $L^{-1}$) (Table 1), undoubtedly a reflection of phytoplankton uptake (see above). At a depth of 10 m, two notable $PO_4$–P local maxima were apparent (Fig. 3d). One was located in the northern upwelling area, where $PO_4$–P concentrations were 0.7–1.0 μmol $L^{-1}$, and even >1.0 μmol $L^{-1}$ in the center of upwelling. Another local maximum was located in the southwest part (122°00′–122°15′ E, 30°45′–31°00′ N) of the study area, where $PO_4$–P concentrations were >1.1 μmol $L^{-1}$ and were probably released from the suspended particulate matter (SPM) in the north of Hangzhou Bay, where tides, such as the famous Qiantang tide, are exceptional (Shen et al. 2008). In the bottom layer, a single area of phosphate-rich water was apparent in the area of upwelling (Table 1, figure not shown), with elliptical isolines corresponding to $PO_4$–P concentration >1.0 μmol $L^{-1}$ and semienclosed isolines associated with $PO_4$–P concentrations of 0.8–0.9 μmol $L^{-1}$.

Throughout most of the study area, and certainly at depths greater than 10 m, physical processes and the high concentrations of nutrients in source waters (i.e., CDW and upwelled water) largely determined the distributions of $NO_3$–N and $SiO_3$–Si. Thus, surface water $NO_3$–N and $SiO_3$–Si concentrations generally declined in an onshore–offshore direction (Fig. 3e, f). However, there was a local minimum of 10–15 μmol $L^{-1}$ in surface water $NO_3$–N concentrations (Fig. 3e) near the center of upwelling. This minimum appears attributable to phytoplankton uptake. Chl-*a* concentrations peaked in the same area at 10–14 μg $L^{-1}$. These high Chl-*a* values would be associated with a phytoplankton biomass of 5–7 μmol $L^{-1}$ (see above) and could thus easily account for the local minimum in nitrate concentrations. A

**Table 1** Spatial variations of T, S, DO, nutrient concentrations, and nutrient ratios in all layers of upwelling in spring and summer

| Months | Layers | T | S | DO | $NO_3$–N | $PO_4$–P | $SiO_3$–Si | DIN:P | Si:DIN | Si:P | Chl–a |
|---|---|---|---|---|---|---|---|---|---|---|---|
| | | °C | | mg $L^{-1}$ | μmol$L^{-1}$ | μmol$L^{-1}$ | μmol$L^{-1}$ | | | | μg $L^{-1}$ |
| May | 0 m | 19.8–20.8 | 24–30 | 4–6 | 10–30 | 0.4–0.6 | 15–30 | 30–70 | 0.8–1.5 | 30–45 | 1–19.5 |
| | 10 m | <16.5–18 | 24–32.5 | < 2.5–3.5 | 10–20 | 0.7–1.1 | 10–20 | < 20–30 | 0.7–1.5 | <15–25 | 1–16.6 |
| | 20 m | 16.2–16.6 | 31–34 | 2–2.8 | 10–15 | 0.7–1.1 | 10–18 | 15–22 | 0.8–1 | 12–25 | 0.15–0.5 |
| | Bottom | ≤16.5 | 31–34 | < 2.5 | 10–20 | 0.8–1.1 | 10–20 | 20–30 | 0.7–1 | 10–25 | 0.25–0.5 |
| August | 0 m | 25.8–26.2 | 14–30 | 6.4–7.2 | 5–50 | 0.4–0.6 | 20–100 | 20–70 | 2.2–3 | 40–160 | 0.5–2.5 |
| | 10 m | 24–25.4 | 24–32 | 3.5–5.5 | 3–20 | 0.4–0.6 | 15–40 | 5–45 | 1.6–3 | 15–70 | 0.5–1 |
| | 20 m | 21.6–24 | 28–34 | < 2.5–4 | 3–10 | 0.7–1.2 | 15–30 | 10–20 | 2.3–3 | 20–40 | 0.1–0.5 |
| | Bottom | 22–23.5 | 28–34 | < 2.5–4 | 5–15 | 0.7–1.4 | 25–40 | 10–20 | 2.4–2.6 | 20–40 | 0.5 |

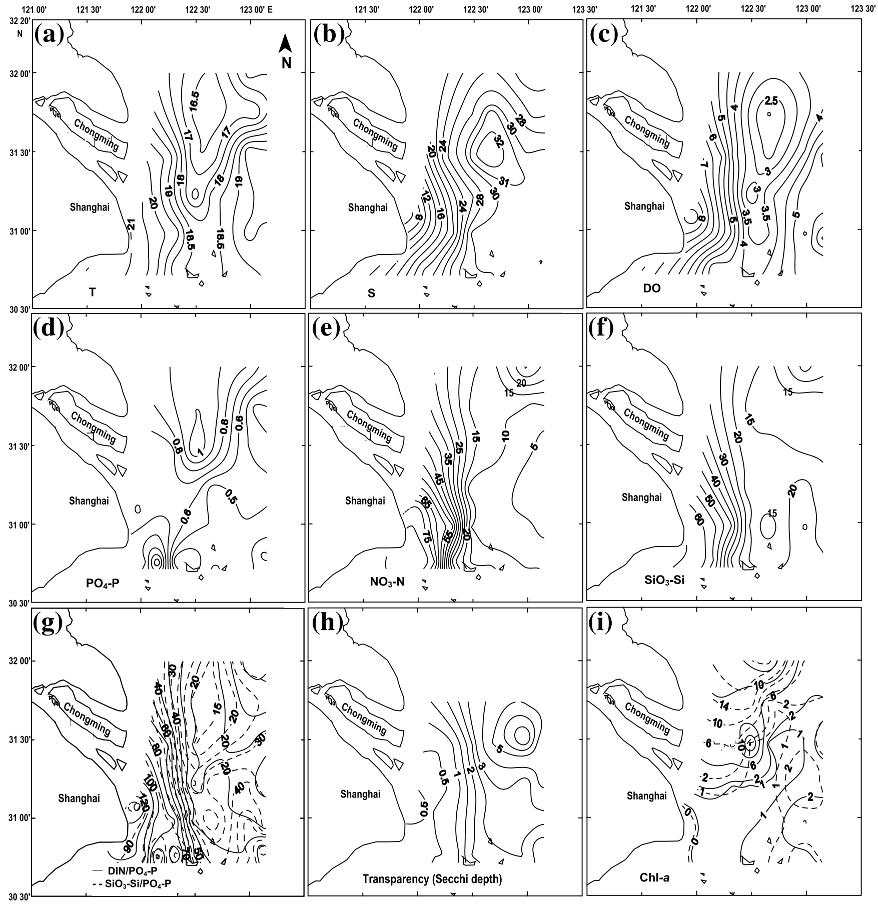


**Fig. 3** Horizontal distributions of T, S, DO, nutrients, nutrient ratios, transparency (Secchi depth), and Chl-*a* in spring: **a** T (°C); **b** S; **c** DO(mg $L^{-1}$); **d** $PO_4$–P (μmol $L^{-1}$); **e** $NO_3$–N (μmol $L^{-1}$); **f** $SiO_3$–Si (μmol $L^{-1}$); **g** DIN: $PO_4$–P(—), $SiO_3$–Si: $PO_4$–P (----); h transparency (Secchi depth [m]); i Chl-*a* (μg $L^{-1}$) in the surface layer (—) and in the 10 m layer (----)

local minimum in surface water $SiO_3$–Si concentrations (< 15 μmol $L^{-1}$) in roughly the same area (Fig. 3f) may also reflect biological uptake. Under nutrient-replete conditions, the Si: N atomic ratio in diatoms is about 1 (Brzezinski 1985). If diatoms accounted for most of the high Chl-*a* biomass, then the associated uptake of $NO_3$–N and $SiO_3$–Si should be roughly equal.

The patterns of DIN: $PO_4$–P and $SiO_3$–Si: $PO_4$–P (Fig. 3g) both show local minima near the center of upwelling. These minima reflect the lower DIN: $PO_4$–P and $SiO_3$–Si: $PO_4$–P ratios in the upwelled water than in the CDW (Fig. 2g, i). With the exception of these local minima, DIN: $PO_4$–P and $SiO_3$–Si: $PO_4$–P ratios declined in an onshore–offshore direction, a reflection of the higher DIN: $PO_4$–P and $SiO_3$–Si: $PO_4$–P ratios in the CDW than in the offshore waters of the East China Sea.

### 2.3 *Chlorophyll-***a** *Distribution in Spring*

The roughly twofold difference in Chl-*a* concentrations between the mouth of the Changjiang River (~5–10 μg $L^{-1}$) and the center of upwelling (15–20 μg $L^{-1}$) (Fig. 3i) appears to reflect largely physical factors because inorganic nutrient concentrations in both areas were more than adequate to support rapid phytoplankton growth. Near the river mouth, Secchi depths were only ~0.5 m (Fig. 3h), which means that the depth of the euphotic zone (1% irradiance) was only ~1.4 m. Clearly, photosynthetic rates were severely light-limited near the river mouth, a conclusion consistent with the earlier study of Chen et al. (2003). In the upwelling area, on the other hand, Secchi depths ranged between 1.5 and >4.9 m, implying euphotic zone depths of 4 to >13 m. Thus, there was considerably less light limitation in the vicinity of the upwelling. Compounding the effect of slow growth rates in the mouth of the river is the increasingly rapid rate of river discharge, from 18,000 $m^3$ $s^{-1}$ in April to 35,700 $m^3$ $s^{-1}$ in June. The increase in discharge would tend to flush slowly growing cells out to sea.

## 3 Nutrient Dynamics of the Upwelling Area in Summer

Previous numerical studies (Zhu 2003; Zhu et al. 2003b) have suggested the existence of upwelling along the west side of the Changjiang submarine river valley in summer, driven mainly by the TWC as it ascends the submarine slope of the East China Sea. However, the numerical study of Pan and Sha (2004) has indicated that the greater the CDW discharge, the weaker the upwelling in the estuary. The Changjiang River discharge in August averages 43,000 $m^3$ $s^{-1}$ (Chen et al. 2003) and in August of 2004 was considerably higher than in May. The resultant vertical salinity gradient depressed upwelling. A comparison of temperature isotherms in spring and summer (Figs. 2a and 4a) reveals that the temperature difference between the surface and upwelled water was about the same (~3 °C) in both seasons. However, along Transect C, salinity in the upper 10 m of the water column over the submarine slope was about 3–5 lower in summer than in spring (Fig. 4b vs. Figure 2b), and during the summer, water containing less than 4 mg $L^{-1}$ DO never penetrated shallower than 10 m (compare Figs. 2c and 4c). Summer upwelling was clearly weaker than spring upwelling in 2004, although the size and flow of the TWC in summer were much greater (Bai and Hu 2004; Jan and Chao 2003; Zhang and Wang 2004). Summer upwelling in 1985 (Zhao et al. 2001) penetrated to shallower depths than in 2004; the difference may reflect annual variations in ocean currents.

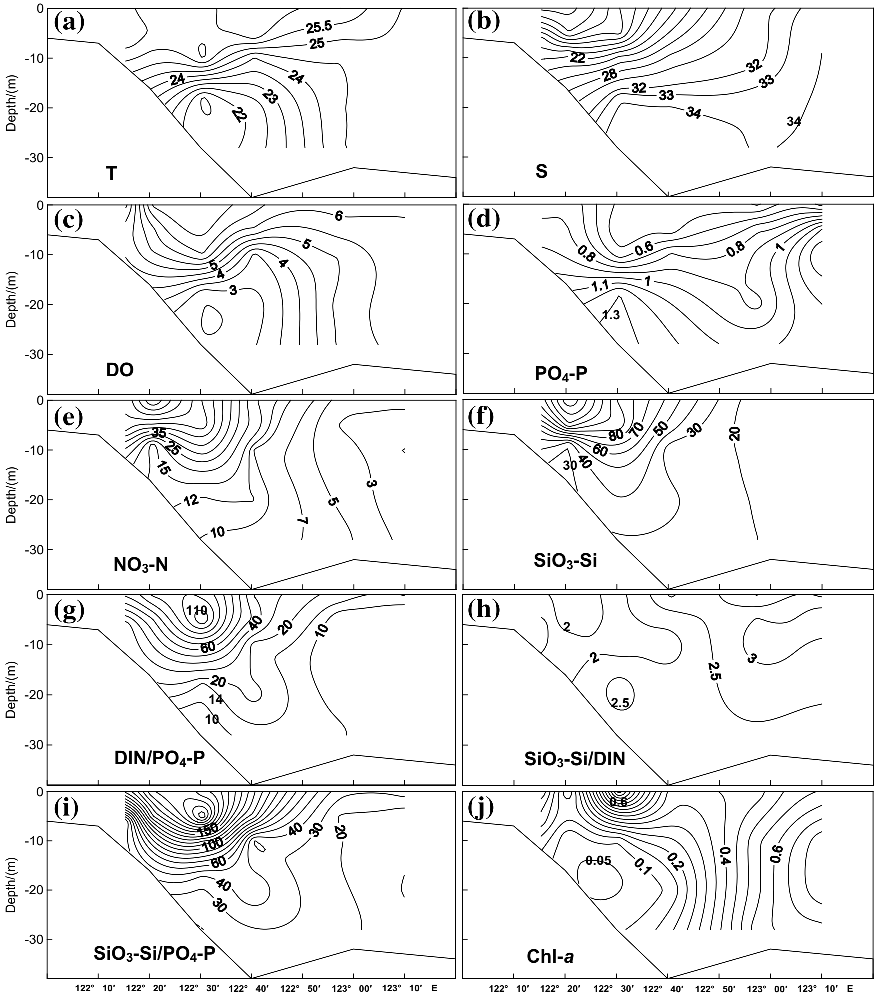


**Fig. 4** Vertical distributions of T, S, DO, nutrients, nutrient ratios, and Chl-*a* in Transect C in summer. **a** T (°C); **b** S; **c** DO (mg $L^{-1}$); **d** $PO_4$–P (μmol $L^{-1}$); **e** $NO_3$–N (μmol $L^{-1}$); **f** $SiO_3$–Si (μmol $L^{-1}$); **g** DIN: $PO_4$–P; **h** $SiO_3$–Si:DIN; **i** $SiO_3$–Si: P $O_4$–P; **j** Chl-*a* (μg $L^{-1}$)

## *3.1 Vertical Distribution of Nutrient*

As in the spring, upwelling during the summer was very apparent along 122°20′–123°00′ E (Fig. 4). However, the salinity gradient in the upper water column prevented upwelled water from penetrating shallower than ~10 m. The doming of nutrient isolines indicates that summer upwelling carried TWC waters to depths of 10–15 m (Fig. 4d, f). However, the concentrations of $NO_3$–N and $SiO_3$–Si in the upwelled water were clearly less than the corresponding concentrations in the

CDW (Fig. 4e, f). The upwelled water contained higher nutrient concentrations than the CDW only in the case of $PO_4$–P. Isolines of $PO_4$–P progressed upslope east of 122°20′ E (Fig. 4d) and reached concentrations of 1.0–1.3 μmol $L^{-1}$ at depths of 15–25 m, much higher than in the surface waters (~0.5 μmol $L^{-1}$). Concentrations of $NO_3$–N and $SiO_3$–Si decreased with increasing depth over the slope, reflecting higher nutrients concentrations in the CDW than in the upwelled water. This pattern contrasts with the distribution of nutrients reported by Zhao et al. (2001) during the summer of 1985, when upwelled waters contained higher concentrations of all nutrients relative to the CDW and surrounding waters. This undoubtedly reflects the roughly threefold increase in DIN and $PO_4$–P concentrations in the Changjiang River between 1985 and 2004 (Wang 2006).

## 3.2 *Horizontal Distribution of Nutrient*

Driven by the upslope flow of the TWC, upwelled waters intruded onshore from 122°25′ E to 122°20′ E. This is apparent not only in Transect C (Fig. 4) but also in horizontal isolines of T, S, and DO at different depths (Fig. 5). In the bottom layer, upwelled waters were apparent to the east of 122°25′ E as semienclosed isolines of low T, high S, and low DO. Temperature in the central upwelling area was <22 °C, 3 °C lower than in the surrounding water (Fig. 5a). The 34 isohaline extended shoreward in a tongue-like shape, evidence of the intrusion of high-salinity upwelled water (Fig. 5b). Dissolved oxygen concentrations in the upwelling area were <2.5 mg $L^{-1}$, compared with 5 mg $L^{-1}$ in surrounding waters (Fig. 5c). At a depth of 20 m, upwelling was evidenced by semienclosed isolines of low T and low DO (Table 1, figure not shown). The area of cooler water became noticeably smaller at shallower depths. In the upper 10 m of the water column, few hydrological effects associated with upwelling were observed, but a local minimum in temperature (25.8–26.2 °C) was apparent at the surface in the area 122°10′–122°40′ E, 31°10′–31°45′ N (Fig. 5a). This likely reflects the divergent flow of surface waters in response to the upwelling. Similar cases of cold surface waters during the summer have been recorded many times by satellite remote sensing in the past (Zhu 2003).

At the surface, $PO_4$–P concentration decreased in an onshore–offshore direction, similar to the pattern observed during the spring (Figs. 3d and 5d). Surface $PO_4$–P concentrations were highest near the river mouth (~1.4 μmol $L^{-1}$), comparable to the values observed in the bottom layer in the upwelling area but clearly higher than the surface water $PO_4$–P concentrations in the vicinity of upwelling. In this case, phytoplankton uptake had little impact on inorganic nutrient concentrations. Peak Chl-*a* concentrations were only ~4 μg $L^{-1}$, which would imply uptake of roughly 2 μmol $L^{-1}$ DIN and 0.125 μmol $L^{-1}$ $PO_4$–P.

In all horizontal layers, the concentrations of $NO_3$–N and $SiO_3$–Si decreased from the river mouth to the open sea eastward (Fig. 5e, f). Because of the strong influence of the nutrient-rich CDW, surface concentrations of $NO_3$–N and $SiO_3$–Si were high in the river mouth, 60–75 μmol $L^{-1}$ and 100–140 μmol $L^{-1}$, respectively.

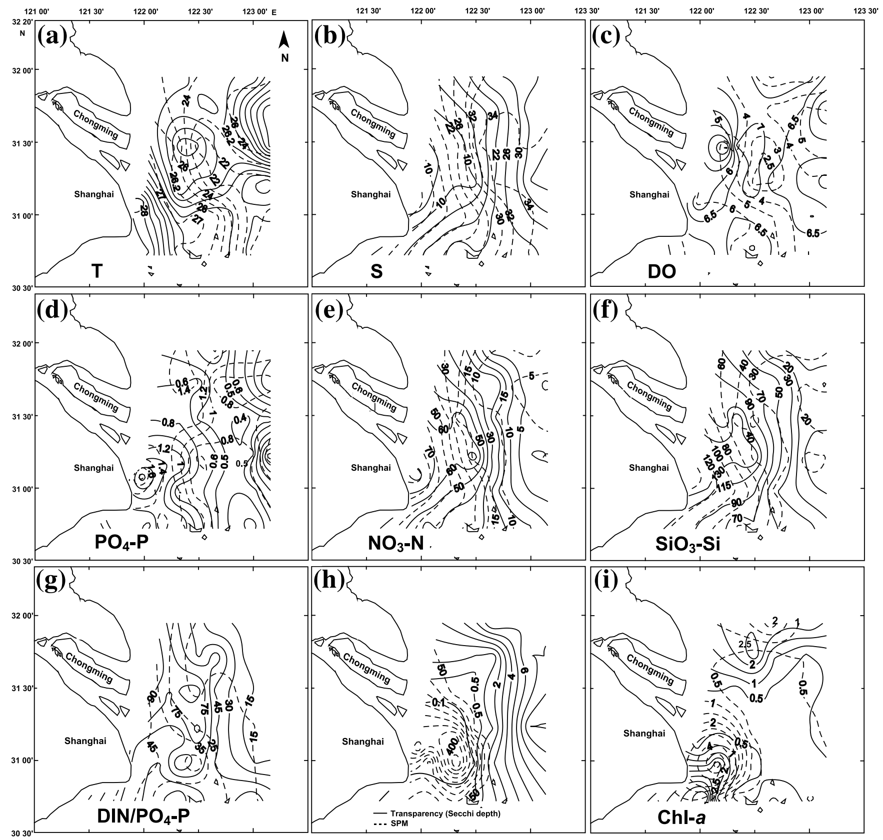


**Fig. 5** Horizontal distributions of T, S, DO, nutrients, nutrient ratio, transparency (Secchi depth), suspended particulate matter (SPM), and Chl-*a* in summer. **a** T (°C); **b** S; **c** DO (mg $L^{-1}$); **d** $PO_4$–P ($\mu$mol $L^{-1}$); **e** $NO_3$–N ($\mu$mol $L^{-1}$); **f** $SiO_3$–Si ($\mu$mol $L^{-1}$); **g** DIN: $PO_4$–P; (**a–g** in the surface layer [—], in the bottom layer [----]); **h** transparency (—) (Secchi depth [m]), SPM (----) (mg $L^{-1}$); i Chl-*a* ($\mu$g $L^{-1}$) (in the surface layer [—], in the 10 m layer [----])

Corresponding surface concentrations in the upwelling area were 5–50 $\mu$mol $L^{-1}$ and 20–100 $\mu$mol $L^{-1}$. From 10 m to the bottom in the upwelling area, $NO_3$–N and $SiO_3$–Si concentrations ranged from 3 to 20 $\mu$mol $L^{-1}$ and 15 to 40 $\mu$mol $L^{-1}$, respectively (Table 1).

The foregoing analysis indicates that upwelling during the summer occurred below 10 m primarily in the region 122°20′–123°00′ E, 31°15′–31°50′ N. Throughout the study area, the nutrient distributions of $PO_4$–P, $NO_3$–N, and $SiO_3$–Si in the surface layer were controlled by the CDW (Fig. 5d, f). Below 10 m, they were influenced considerably by upwelling.

### 3.3 *Chlorophyll-*a *Distribution in Summer and Its Seasonal Difference*

Inorganic nutrient concentrations in the upper 10 m of the water column were clearly adequate to support phytoplankton blooms, but the highest Chl-*a* concentrations in the upwelling area were only ~0.5–1.0 μg $L^{-1}$ (Figs. 4j and 5i). Surface water $PO_4$–P concentrations were at least 0.4 μmol $L^{-1}$, which is adequate to support a phytoplankton biomass of ~13 μg $L^{-1}$ Chl-*a* (see above). Nitrate and $SiO_3$–Si were present in even greater abundance relative to the needs of phytoplankton. Dissolved inorganic nitrogen: $PO_4$–P was above 60 (Figs. 4g and 5g); $SiO_3$–Si: DIN was from 2 to 2.4 (Fig. 4h), and $SiO_3$–Si: $PO_4$–P was from 100 to 160 (Fig. 4i). Clearly, phytoplankton biomass was not nutrient-limited. Why was the phytoplankton biomass so much higher in the spring than in the summer?

The answer appears to be extreme light limitation during the summer upwelling period. Secchi depths in the upwelling area were only ~0.5 m in the summer (Fig. 5h), the depth of the euphotic zone, therefore, being only about 1.4 m. Surface Chl-a concentrations increased from 0.5 to 2.5 μg $L^{-1}$ at 31°30′ N (Fig. 5i), where Secchi depths were greater than 5 m. The low transparency during the summer was caused by the strong discharge of low salinity and turbid waters from the CDW (SPM is 50 to >400 mg $L^{-1}$) (Fig. 5h), which overflowed clearer TWC waters and prevented upwelling from penetrating to depths shallower than 10 m.

## 4 Compared the Spring Upwelling with the Summer Upwelling

Spatial variations of hydrological parameters in the upwelling area in spring and summer are summarized in Table 1.

In the spring, upwelling was apparent in the region of 122°20′–123°00′ E, 31°00′–32°00′ N and was characterized by low temperature (16–21 °C), high salinity (24–33), and low DO (2.5–6.0 mg $L^{-1}$) in the upper 10 m of the water column. The spring upwelling increased mixed-layer $PO_4$–P, $NO_3$–N, $SiO_3$–Si concentrations and improved light transparency in the euphotic zone. This improvement in phytoplankton-growing conditions was followed by an increase in Chl-*a* concentrations. The summer upwelling was weaker and occurred over a smaller geographical area (122°20′–123°00′ E, 31°15′–31°50′ N). Strongly influenced by turbid CDW, it had little impact on the upper 10 m of the water column but, instead, increased nutrient concentrations at greater depths.

The impact of upwelling on phytoplankton biomass over the submarine slope offshore of the Changjiang River is modulated very much by the discharge of turbid water from the river. During May 2004, the depth of the euphotic zone in the mouth of the river was only ~1.4 m, and phytoplankton biomass was very much constrained by light limitation. The plume of turbid CDW, however, did not extend far enough from shore to restrict upwelling or prevent a bloom of phytoplankton from developing in the vicinity of 122°20′ E, where the depth of the euphotic zone was 4–13 m. By August 2004, the plume of turbid CDW extended far enough from shore to prevent upwelled waters from reaching the euphotic zone, which was only ~1.4 m deep.

# 5 Estimation of Nutrient Fluxes in the Spring Upwelling

Our foregoing analyses suggest that coastal upwelling was most obvious in spring and carried rich phosphate but relatively low-content nitrate and silicate into the upper layers, which optimized local nutrient supplies to a relatively large extent and thus stimulated the growth of phytoplankton. However, compared with the Changjiang runoff, which one carried a higher concentration of nutrients? And which one had a more significant impact? Little study has been carried out on these questions. Nutrient fluxes of spring upwelling were estimated in this section and were compared with the historical data of the nutrient fluxes from the Changjiang runoff in order to provide valuable references for the future study of eutrophication and the mechanism of red tides.

## *5.1 Calculation Method and Result*

In this section, we followed the method reported by Chen and Ruan (1996) for the estimation of nutrient fluxes in the upwelling area of Taiwan Strait to estimate the vertical fluxes of nitrogen, phosphorus, and silicon in the upwelling area of the Changjiang estuary. The equation is:

$$P = a \cdot C \cdot W \tag{1}$$

where $P$ (g m$^{-2}$ d$^{-1}$) is the nutrient vertical flux from the bottom into the upper layer carried by upwelled water, a is a unit conversion factor, $C$ (μmol L$^{-1}$) is the concentration of nutrient, and $W$ (m s$^{-1}$) is the speed of upwelling.

Since the upwelling speed ranged between $1.0 \times 10^{-5}$–$5.0 \times 10^{-5}$ m s$^{-1}$ according to the calculation of Zhao (1993), the nutrient vertical fluxes can be estimated as a range accordingly. In addition, the upwelling region and its corresponding average nutrient concentrations are able to be calculated in accordance with the nutrient distributions which were influenced significantly by upwelling at the 10 m depth. The estimated ranges of nutrient fluxes (kg s$^{-1}$) by Eq. (1) are listed in Table 2.

The estimation of $PO_4$–P vertical flux was calculated individually for four subzones defined by the variation of average concentration in the layer of 10 m, and then the total $PO_4$–P flux at the 10 m depth was calculated to be 1.4–7.0 kg s$^{-1}$ (or

**Table 2** Comparison nutrient vertical fluxes in the upwelling area with input fluxes from the Changjiang runoff

| Nutrients | Areas | Average concentrations | Speeds | Vertical fluxes | Fluxes | Changjiang runoff Shen (1993) |
|---|---|---|---|---|---|---|
| | $\times 10^6$ m$^2$ | μmol L$^{-1}$ | $\times 10^{-5}$m s$^{-1}$ | mg m$^{-2}$ d$^{-1}$ | kg s$^{-1}$ | kg s$^{-1}$ |
| $PO_4$–P | 268.53 | 1.0 | 1–5 | 26.76–133.8 | 1.4–7.0 | 0.43 |
| | 2612.02 | 0.95 | 1–5 | 25.42–127.1 | | |
| | 1379.25 | 0.85 | 1–5 | 22.75–113.75 | | |
| | 805.58 | 0.75 | 1–5 | 20.07–100.35 | | |
| $SiO_3$–Si | 5065.37 | 14.62 | 1–5 | 354.77–1773.85 | 20.8–104 | 63.3 |
| $NO_3$–N | 5065.37 | 13.38 | 1–5 | 161.92–809.6 | 9.49–47.45 | 20.0 |
| DIN | 5065.37 | 16.42 | 1–5 | 198.71–993.55 | 11.65–58.25 | 27.9 |

23.91–119.57 mg m$^{-2}$ d$^{-1}$) by the weighted sum for four subzones. Our estimation is obviously higher than 10.03–50.16 mg m$^{-2}$ d$^{-1}$ reported by Yang et al. (2005) according to the investigation result of East China Sea in 1998.

## 5.2 *Nutrient Fluxes Comparison*

The estimated $PO_4$–P flux above in the spring upwelling was much higher than the Changjiang runoff inputting calculated by Shen (1993) based on investigations during 1985 and 1986 (Table 2), and the estimated minimum was more than twice higher than the flux from the Changjiang runoff, which might affect the distribution of $PO_4$–P and the growth of phytoplankton and therefore become a factor worth paying attention to. Comparatively, the fluxes of $SiO_3$–Si, $NO_3$–N, and DIN were less in the upwelled water, since their minima only accounted for 33.3, 47.6 and 41.7%, respectively, of the corresponding fluxes from the Changjiang runoff. It is noteworthy that only nutrient fluxes in spring were calculated in this chapter, and it is possible that the nutrient fluxes in spring were higher than the annual average nutrient fluxes in the upwelling area. Calculated results above are consistent with the observation of nutrient distribution patterns. The upwelled water with high $PO_4$–P but relatively low $NO_3$–N and $SiO_3$–Si were able to change the nutrient structure in this area and subsequently impacted on the phytoplankton growth. Our current results show that the ratios of nutrient fluxes in the upwelling to those from the Changjiang runoff ranged 3.3–16.2, 0.33–1.6, 0.47–2.4 and 0.42–2.1 for $PO_4$–P, $SiO_3$–Si, $NO_3$–N, and DIN, respectively (Table 2). So many amounts of nutrients, especially $PO_4$–P, were carried from the bottom into the upper layers by the upwelled water that upwelling becomes one of the major nutrient sources in the studied area and probably exerts an

**Table 3** Comparison nutrient fluxes (mg m$^{-2}$ d$^{-1}$) in the upwelling area of the Changjiang River estuary with other coastal upwelling areas (Chen and Ruan 1996)

| Nutrients | Changjiang estuary | Zhoushan and Yushan Fisheries | Middle and north Taiwan Strait | Southern Fujian and Taiwan Shallow fisheries | Zhejiang coastal | East Guang-dong coastal |
|---|---|---|---|---|---|---|
| $PO_4$–P | 23.91–119.57 | 38–189 | 23.6 | 13.2 | | 46.5 |
| $SiO_3$–Si | 354.77–1773.85 | 669–3348 | 302 | 264 | | |
| $NO_3$–N | 161.92–809.6 | 165–824 | 223 | 88.5 | 33.87–2143.7 | |
| years | 2004 | 1984 | 1988 | 1988 | 1981 | |
| References | This section | Wang and Zang (1987) | Chen and Ruan (1996) | Wu and Ruan (1991) | Lei (1984) | Han and Ma (1988) |

impact that cannot be ignored on the eutrophication in the Changjiang River estuary. Of course, it is different in nutrient fluxes from the Changjiang runoff in different years. Previous study showed that there were clear positive relationships between the nutrient export fluxes in the Changjiang mouth and the river's runoff (Shen 1993; Shen et al.2003, 2009). Therefore, the nutrient fluxes from the Changjiang runoff change with the change of the Changjiang runoff. For example, in 1998 of especially heavy flood, the $PO_4$–P, $NO_3$–N, and DIN fluxes from the Changjiang runoff were 0.74, 45.59, and 55.38 kg s$^{-1}$, respectively, being 1.7, 2.3, and 2.0 times of those in 1985–1986.

Comparison of nutrient fluxes in the upwelling area of the Changjiang River estuary with other upwelling areas (Table 3) shows that all calculated results are of the same order of magnitude. The nutrient fluxes in the upwelling areas of Zhoushan Fishery and Yushan Fishery were relatively high, and fluxes were relatively high in the upwelling area of Changjiang River estuary as well, compared with other coastal upwelling areas.

## References

Bai, X. Z., & Hu, D. X. (2004). A numerical study on seasonal variations of the Taiwan Warm Current. *Chinese Journal of Oceanology and Limnology, 22,* 278–285.

Barber, R. T., & Smith, R. L. (1981). Coastal upwelling ecosystems.In A. R. Longhurst (ed.), *Analysis of marine ecosystems* (pp. 31–68). London, U.K.: Academic Press.

Beardsley, R. C., Limeburner, R., Le, K. T., Hu, D. X., Cannon, G. A., & Pashinski, D. J. (1983). Structure of the Changjiang river plume in the East China Sea during June 1980. In Acta Oceanologica Sinica (eds.), *Proceedings of the international symposium on sedimentation on the continental shelf, with special reference to the East China Sea*, (Vol. 1, pp. 265–284). Hangzhou, China: China Ocean Press.

Blasco, D., Estrada, M., & Burton, J. (1980). Relationship between the phytoplankton distribution and composition and the hydrography in the northwest African upwelling region near Cabo Corbeiro. *Deep-Sea Research, 27A,* 799–821.

Blasco, D., Estrada, M., & Jones, B. H. (1981). Short time variability of phytoplankton populations in upwelling regions-the example of Northwest Africa. In F. Richard (ed.), *Proceedings of the inter-national symposium on coastal upwelling* (pp. 339–347). Los Angeles, California: American Geophysical Union.

Brzezinski, M. A. (1985). The Si: C: N ratio of marine diatoms: Interspecific variability and the effect of some environmental variables. *Journal of Phycology, 21,* 347–357.

Chen, S. T., & Ruan, W. Q. (1996). Chemical characteristics of N, P and Si in the upwelling area of Taiwan Strait and the estimation of their fluxes. *Acta Oceanologica Sinica, 18*(3), 36–44. (in Chinese with English abstract).

Chen, Y. L. L., Chen, H. Y., Gong, G. C., Lin, Y. H., Jan, S., & Taka-hashi, M. (2004). Phytoplankton production during a summer coastal upwelling in the East China Sea. *Continental Shelf Research, 24,* 1321–1338.

Chen, Y. L. L., Lu, H., Shiah, F., Gong, G., Liu, K., & Kanda, J. (1999). New production and f-ratio on the continental shelf of theEast China Sea: comparisons between nitrate inputs from the sub-surface Kuroshio Current and the Changjiang River. *Estuarine, Coastal and Shelf Science, 48,* 59–75.

Chen, C., Zhu, J., Beardsley, R. C., & Franks, P. J. S. (2003). Physical-biological sources for dense algal blooms near the Changjiang River. *Geophysical Research Letters, 30*(10), 1515.

Chen-Tung, A., & Sheu, D. D. (2006). Does the Taiwan Warm Current originate in the Taiwan Strait in wintertime? *Journal of Geophysical Research, 111,* C04005.

Cui, A., & Street, R. (2004). Large-eddy simulation of coastal upwelling flow. *Environmental Fluid Mechanics, 4,* 197–223.

Gao, X. L., & Song, J. M. (2005). Phytoplankton distributions andtheir relationship with the environment in the Changjiang Estuary, China. *Marine Pollution Bulletin, 50,* 327–335.

Guo, B. H., Hu, X. M., Xiong, X. J., & Ge, R. F. (2003). Study on interaction between the coastal water, shelf water and Kuroshio water in the Huanghai Sea and East China Sea. *Acta Oceanologica Sinica, 22,* 351–367.

Han, W. Y., & Ma, K. M. (1988). The study of coastal upwelling along East Guangdong. *Acta Oceanologica Sinica, 10*(1), 52–59 (in Chinese)

Hu, D. (1994). Some striking features of circulation in Huanghai Sea and East China Sea. In D. Zhou, Y. B. Liang, & C. K. Tseng (Eds.), *Oceanology of China Seas* (Vol. 1, pp. 27–38). Dordrecht, the Netherlands: Kluwer Academic Publishers.

Jan, S., & Chao, S. Y. (2003). Seasonal variation of volume transportin the major inflow channel of the Taiwan Strait: Penghu Channel. *Deep-Sea Research, Part 2: Topical Studies in Oceanography, 50*(6), 1117–1126.

Katoh, O., Morinaga, K., & Nakagawa, N. (2000). Current distributions in the southern East China Sea in summer. *Journal of Geophysical Research, 105*(C4), 8565–8573.

Lei, P. F. (1984). Calculations of speed and nutrient fluxes of coastal upwelling in Zhejiang. *Transactions of Oceanology and Limnology, 2,* 22–26 (in Chinese with English abstract)

Limeburner, R., Beardsley, R. C., & Zhao, J. S. (1983). Water massesand circulation in the East China Sea. In Acta Oceanologica Sinica (eds.), *Proceedings of the international symposium on sedimentation on the continental shelf, with special reference to the East China Sea*, (Vol. 1, pp. 285–294). Hangzhou, China: China Ocean Press.

Margalef, R. (1978a). Phytoplankton communities in upwelling areas: the example of NW Africa. *Oecologica Aquatica, 3,* 97–132.

Margalef, R. (1978b). Life-forms of phytoplankton as survival alter-natives in an unstable environment. *Oceanologica Acta, 1,* 493–509.

Naimie, C. E., Blain, C. A., & Lynch, D. R. (2001). Seasonal mean circulation in the Yellow Sea—a model-generated climatology. *Continental Shelf Research, 21,* 667–695.

Oleg, Z., Rafael, C. D., Orzo, M., & Assrtemio, G. G. (2003). Coastalupwelling activity on the Pacific Shelf of the Baja California Peninsula. *Journal of Oceanography, 59,* 489–502.
Pan, Y. P., & Sha, W. Y. (2004). Numerical study on the summercoastal upwelling off Fujian and Zhejiang. *Marine Science Bulletin, 23,* 1–11.
Ramírez, T., Cortés, D., Mercado, J. M., Vargas-Yanez, M., Sebastián, M., & Liger, E. (2005). Seasonal dynamics of inorganic nutrients and phytoplankton biomass in the NW Alboran Sea. *Estuarine, Coastal and Shelf Science, 65*(4), 654–670.
Redfield, A. C., Ketchum, B. H., & Richards, F. (1963). The influence of organisms on the composition of seawater. In M. N. Hill (Ed.), *The Sea* (Vol. 2, pp. 26–77). New York: John Wiley.
Riemann, B., Simonsen, P., & Stensgaard, L. (1989). The carbonand chlorophyll content of phytoplankton from various nutrientregimes. *Journal of Plankton Research, 11,* 1037–1045.
Ryther, J. H. (1969). Photosynthesis and fish production in the sea. *Science, 166,* 72–76.
Shen, Z. L. (1993). A study on the relationships of the nutrients near the Changjiang River estuary with the flow of the Changjiang River water. *Chinese Journal Oceanology and Limnology, 11,* 260–267.
Shen, Z. L., & Liu, Q. (2009). Nutrients in the Changjiang River. *Environmental Monitoring and Assessment, 153*(1), 27–44.
Shen, Z. L., Liu, Q., Wu, Y. L., & Yao, Y. (2006). Nutrient structure of seawater and ecological responses in Jiaozhou Bay, China. *Estuarine, Coastal and Shelf Science, 69*(1–2), 299–307.
Shen, Z. L., Liu, Q., Zhang, S. M., Miao, H., & Zhang, P. (2001). The dominant controlling factors of high content inorganic nitrogen in the Changjiang river and its mouth. *Oceanologia et Limnologia Sinica, 32,* 465–473. (in Chinese with English abstract).
Shen, Z. L., Liu, Q., & Zhang, S. M., Miao, H., & Zhang, P. (2003). A nitrogen budget of the Changjiang River catchment. *Ambio, 32*(1), 65–69.
Shen, Z. L., Zhou, S. Q., & Pei, S. F. (2008). Transfer and transport of phosphorus and silica in the turbidity maximum zone of the Changjiang estuary. *Estuarine, Coastal and Shelf Science, 78*(3), 481–492.
Skliris, N., & Djenidi, S. (2006). Plankton dynamics controlled by hydrodynamic processes near a submarine canyon off NW Corsican coast: a numerical modelling study. *Continental Shelf Re-search, 26,* 1336–1358.
Smith, W. O., Heburn, G. W., Barber, R. T., & O'Brien, J. J. (1983). Regulation of phytoplankton communities by physical processes in upwelling ecosystems. *Journal of Marine Research, 41,* 539–556.
Su, J. (1998). Circulation dynamics of the China Seas north of 18°N coastal segment (12, S). In A. R. Robinson & K. H. Brink (Eds.), *The Sea* (Vol. 11, pp. 483–505). New York: Wiley.
Wang, B. D. (2006). Cultural eutrophication in the Changjiang (Yangtze River) plume: History and perspective. *Estuarine, Coastal and Shelf Science, 69,* 471–477.
Wang, B. D., & Wang, X. L. (2007). Chemical hydrography of coastal upwelling in the East China Sea. *Chinese Journal of Oceanology and Limnology, 25*(1), 16–26.
Wang, G. Y., & Zhang, J. Y. (1987). The contents and distributions of chemical elements in East China Sea. *Collection of Research Papers on the Investigation of the Kuroshio*, (pp. 267–284). Beijing: Ocean Press (in Chinese)
Wu, L. Y., & Ruan, W. Q. (1991). Study on the nutrients in the upwelling area of Southern Fujian and Taiwan Shallow fisheries. *Study on the Ecosystem in the Upwelling Area of Southern Fujian and Taiwan Shallow Fisheries*, (pp. 169–178). Beijing: Science Press (in Chinese with English abstract)
Yang, H., Li, G., & Jin, C. F. (2005). The regeneration and vertical flux of phosphate in the Yangtze River Estuary and its adjacent area. *Journal of Shanghai fisheries University, 14*(2), 162–167. (in Chinese with English abstract).
Yu, H. H., Zheng, D.C., & Jiang, J.Z. (1983). Basic hydrographic characteristics of the studied area. In Acta Oceanologica Sinica (eds.), *Proceedings of the international symposium on sedimentation on the continental shelf, with special reference to the East China Sea*, (Vol. 1, pp. 295–305). Hangzhou, China: China Ocean Press.

Zhang, Q. L., & Wang, F. (2004). Climatological analysis of water masses in Zhoushan fishing ground and adjacent region. *Oceanologia et Limnologia Sinica, 35,* 48–53. (in Chinese with English abstract).

Zhao, B. R. (1993). Upwelling phenomenon off Changjiang estuary. *Acta Oceanologica Sinica, 15,* 106–114. (in Chinese with English abstract).

Zhao, B. R., Le, K. T., & Zhu, L. B. (1992). Characteristics of the temperature and salinity distribution and the upwelling phenomenon in the Changjiang River mouth area. Institute of Oceanology, Chinese Academy of Sciences. Studia Marina Sinica, *33*, pp. 15–26. Beijing: Science Press. (in Chinese with English abstract).

Zhao, B. R., Ren, G. F., Cao, D. M., & Yang, Y. L. (2001). Characteristics of the ecological environment in upwelling area adjacent tothe Changjiang River estuary. *Oceanologia et Limnologia Sinica, 32,* 327–333. (in Chinese with English abstract).

Zhou, M. J., Yan, T., & Zou, J. Z. (2003). Preliminary analysis of the characteristics of red tide areas in Changjiang river estuary and its adjacent sea. *Chinese Journal of Applied Ecology, 14,* 1031–1038. (in Chinese with English abstract).

Zhu, D. D., Pan, Y. Q., Xu, W. Y., & Chen, Q. Y. (2003a). Hydrologic distribution characteristics of HAB frequent occurrence area in the outer Changjiang River estuary. *Chinese Journal of Applied Ecology, 14,* 1131–1134. (in Chinese with English abstract).

Zhu, J. R. (2003). Dynamic mechanism of upwelling in the west of submarine valley in the Changjiang estuary in summer. *Chinese Science Bulletin, 48,* 2488–2492. (in Chinese with English abstract).

Zhu, J. R., Ding, P. X., & Hu, D. X. (2003b). Observation of the diluted water and plume front off the Changjiang river estuary during August 2000. *Oceanologia et Limnologia Sinica, 34,* 249–255. (in Chinese with English abstract).